Donor impurity band exchange in dilute ferromagnetic oxides

J. M. D. COEY*, M. VENKATESAN AND C. B. FITZGERALD
Physics Department, Trinity College, Dublin 2, Ireland
***e-mail: jcoey@tcd.ie**

Published online: 16 January 2005; doi:10.1038/nmat1310

Dilute ferromagnetic oxides having Curie temperatures far in excess of 300 K and exceptionally large ordered moments per transition-metal cation challenge our understanding of magnetism in solids. These materials are high-*k* dielectrics with degenerate or thermally activated n-type semiconductivity. Conventional super-exchange or double-exchange interactions cannot produce long-range magnetic order at concentrations of magnetic cations of a few percent. We propose that ferromagnetic exchange here, and in dilute ferromagnetic nitrides, is mediated by shallow donor electrons that form bound magnetic polarons, which overlap to create a spin-split impurity band. The Curie temperature in the mean-field approximation varies as $(x\delta)^{1/2}$ where x and δ are the concentrations of magnetic cations and donors, respectively. High Curie temperatures arise only when empty minority-spin or majority-spin *d* states lie at the Fermi level in the impurity band. The magnetic phase diagram includes regions of semiconducting and metallic ferromagnetism, cluster paramagnetism, spin glass and canted antiferromagnetism.

The most interesting new magnetic materials to emerge in the last few years are a group of dilute ferromagnetic oxides and nitrides, which are wide-gap semiconductors with Curie temperatures T_C well in excess of room temperature[1,2]. Interest in the field was catalysed by a prediction[3] of room-temperature ferromagnetism in p-type GaN or ZnO doped with 5% Mn. First reports for oxides were for Co-doped thin films of TiO_2 (anatase), ZnO and SnO_2 (refs 4–6, respectively). A list of oxides and nitrides where high-temperature ferromagnetism has been reported is given in Table 1. It is necessary to understand this magnetism in order to develop thin-film magneto-optic and spin-electronic devices that could operate in ambient conditions.

A syndrome, or set of symptoms is associated with the high-temperature ferromagnetism in these films. The oxides are generally n-type, with a high dielectric constant, but they may be partially compensated. Ferromagnetism appears in degenerate or non-degenerate semiconductors, and even in insulators, at concentrations of 3*d* dopants that lie far below the percolation threshold x_p associated with nearest-neighbour cation coupling. The average moment per dopant cation m_c approaches (or even exceeds) the spin-only moment at low dopant concentrations x, and it falls progressively as x increases towards x_p. Finally, properties vary greatly for samples of the same nominal composition prepared by different methods, or by different groups. A compendium of results on the concentration dependence of the ferromagnetic moments in the extensively studied TiO_2, ZnO and SnO_2 systems shown in Fig. 1 illustrates these points.

At first, the results were so unexpected that explanations were sought in terms of phase segregation. Although ferromagnetic impurity phases may be present in some samples, notably of anatase and rutile[7,8], they cannot provide a general explanation[9]. The ordered magnetic moments per 3*d* cation at low concentrations are unprecedented, exceeding those in almost all known oxides or alloys, including the pure metal[10]. Such high moments per cation are inexplicable in terms of possible known ferromagnetic phases.

These results challenge our understanding of magnetism in oxides. Super-exchange, which is predominantly antiferromagnetic and short-ranged[11], cannot be invoked because the magnetic order appears at concentrations of magnetic cations $x < x_p$. In any case the average net moment per magnetic cation in ferrimagnetically ordered superexchange systems is rarely much more than one Bohr

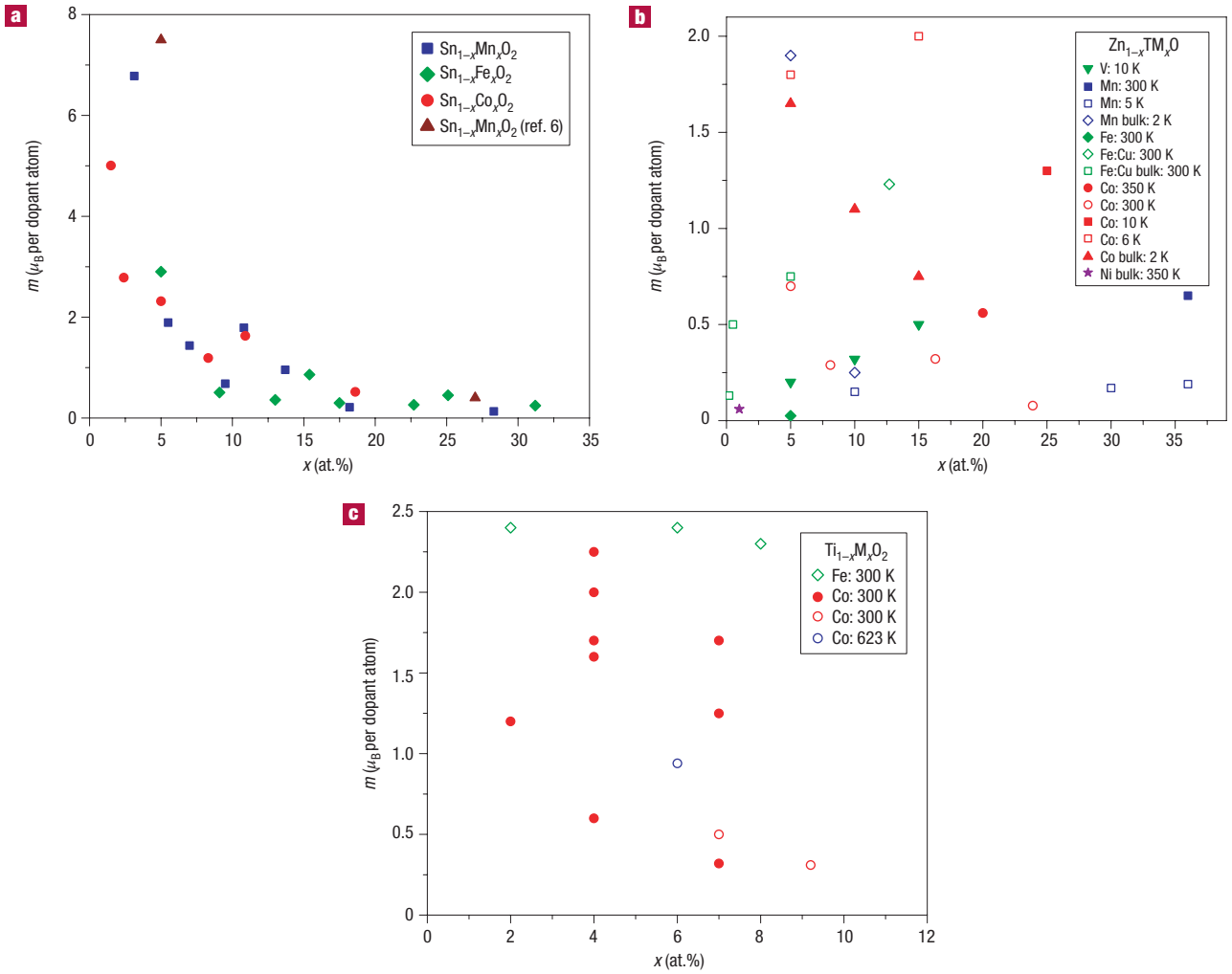

Figure 1 Plots of magnetic moment per transition-metal cation in doped oxide thin films. **a**, SnO_2 doped with Mn, Fe or Co. **b**, ZnO doped with V, Mn, Co, Fe or Ni. **c**, TiO_2 doped with Fe or Co (rutile – open circles; anatase – filled circles). Moments of the cations in their high-spin state are 5 μ_B for Mn^{2+} or Fe^{3+}; 4 μ_B for Mn^{3+}, Fe^{2+} or Co^{3+}; 3 μ_B for Mn^{4+} or Co^{2+}.

magneton (μ_B). The ferromagnetic double-exchange mechanism, as described by Zener with reference to mixed-valence manganites, can produce large moments, but it is also a nearest-neighbour interaction that requires mixed cation valence so that $3d^n \leftrightarrow 3d^{n+1}$ configuration fluctuations can occur. There is no evidence that mixed valence is a common feature of these dilute oxides.

Longer-range ferromagnetic exchange can be mediated by carriers in a spin-polarized band. For example, in Dietl's model, Mn introduces holes in the *p*-band of GaAs or GaN. Well-studied semiconductor examples are: (i) n-type europium monochalcogenides such as EuS, where the carriers are ↑ electrons in the spin-split 5*d*/6*s* conduction band produced by doping with donors such as Gd^{3+}; and the Eu^{2+} $4f^7$ magnetic core level lies in the gap[12]. (ii) p-type III-V dilute magnetic semiconductors such as $(Ga_{1-x}Mn_x)As$ where carriers are ↓ holes in the 4*p* valence band; the Mn^{2+} $3d^5$ core level lies below the top of this band[13].

Curie temperatures in these semiconductors range up to about 170 K, disqualifying them for most practical applications. A Curie temperature of at least 500 K is usually necessary to qualify a ferromagnet for use in a room-temperature device.

IMPURITY-BAND EXCHANGE

Here the ferromagnetic exchange coupling and magnetic moments in dilute n-type oxides are discussed in terms of a simple model, based on the tendency of these materials to form shallow donors. It is shown how a high T_C may be achieved, and some other predictions are made.

The general formula for the oxides is

$$(A_{1-x}M_x)(O\square_\delta)_n \qquad (1)$$

where A is a nonmagnetic cation, M is a magnetic cation, □ represents a donor defect and $n = 1$ or 2. An electron associated with a particular defect will be confined in a hydrogenic orbital of radius $r_H = \varepsilon(m/m^*)a_0$, where ε is the high-frequency dielectric constant, m is the electron mass, m^* is the effective mass of the donor electrons and a_0 is the Bohr radius (53 pm). Values of r_H are listed in Table 2. The binding energy of the donor electron in a 1*s* orbital is $E_B = (m^*/m\varepsilon^2)R_\infty$, where R_∞, the Rydberg constant, is 13.6 eV. The depth of the electron traps is therefore of the order of a few tenths

Table 1 High-temperature ferromagnetism in dilute ferromagnetic oxides and nitrides.

Material	E_g (eV)	Doping x	Moment (μ_B)	T_C (K)	Reference
GaN	3.5	Mn – 9%	0.9	940	34
		Cr	-	>400	35
AlN	4.3	Cr – 7%	1.2	>600	36
TiO_2	3.2	V – 5%	4.2	>400	28
		Co – 1–2%	0.3	>300	4
		Co – 7%	1.4	650–700	37
		Fe – 2%	2.4	>300	38
SnO_2	3.5	Fe – 5%	1.8	610	39
		Co – 5%	7.5	650	6
ZnO	3.3	V – 15 %	0.5	>350	27
		Mn – 2.2%	0.16	>300	40
		Fe – 5%, Cu – 1%	0.75	550	41
		Co – 10%	2.0	280-300	5
		Ni – 0.9%	0.06	>300	42
Cu_2O	2.0	Co – 5%, Al – 0.5%	0.2	>300	43
$In_{1.8}Sn_{0.2}O_3$	3.8	Mn – 5%	0.8	>300	44

of an electron volt. As the donor concentration δ increases, the 1*s* orbitals $\psi(r) = (\pi r_H^3)^{-1/2}\exp(-r/r_H)$, where r is the distance from the nucleus, overlap to form an impurity band. At first, the electrons remain localized because of the influence of correlations and potential fluctuations in a narrow band, but there is a critical donor concentration $n_\square^{crit}$ where the impurity band states become delocalized, and metallic conduction sets in, namely $(n_\square^{crit})^{1/3} r_H \approx 0.26$ (ref. 14). The corresponding value δ^{crit} is $n_\square^{crit}/n_O$, where the oxygen density $n_O \approx 6 \times 10^{28}$ m^{-3} for oxides with a close-packed oxygen lattice. Hence

$$\gamma^3 \delta^{crit} \approx 2.2 \quad (2)$$

where the radius of the orbital $r_H = \gamma a_0$, where $\gamma = \varepsilon(m/m^*)$.

Consider now the interaction of the magnetic cations M with the hydrogenic electrons in the impurity band. The donors tend to form bound magnetic polarons, coupling the 3*d* moments of the ions within their orbits[15–19]. The basic idea is illustrated in Fig. 2. The cations present an extra random potential, which extends the localized region as x increases. Provided the radius of its orbital is sufficiently large, say $\gamma > 4$, overlap between a hydrogenic electron and the cations within its orbit leads to ferromagnetic exchange coupling between them[19]. This interaction may be written in terms of the *s*–*d* exchange parameter J_{sd} as[14]

$$-J_{sd}\mathbf{S}.\mathbf{s}|\psi(r)|^2\Omega \quad (3)$$

where **S** is the spin of the 3*d* cations that have volume Ω, and **s** is the donor electron spin. The number of cation sites v_c within a sphere of radius r_H ranges from ten to a hundred, depending on γ (Table 2). The number of these sites occupied by a magnetic cation is $v = xv_c$. The high-frequency dielectric constant is appropriate for a metallic impurity band, but larger values may apply when the electrons are localized.

In the case of a $3d^5$ ion such as Fe^{3+} or Mn^{2+}, the only unoccupied 3*d* orbitals available are ↓. Hence the donor electron is ↓, and the effective coupling between two magnetic impurities falling within the same donor orbital is ferromagnetic. More generally, the coupling between the cation and the donor electron is ferromagnetic when the 3*d* shell is less than half full, and antiferromagnetic when the 3*d* shell is half full or more. Either way, the coupling between two similar impurities within the same donor orbital is ferromagnetic.

As the density of defects $n_\square$ increases, the hydrogenic orbitals associated with the randomly positioned defects overlap. Approximating them as randomly packed spherical objects, percolation occurs when they fill roughly 16% of space[20]. Expressed in terms of $\delta = n_\square/n_O$ the percolation threshold for the appearance of long-range ferromagnetic order is $\gamma^3\delta_p \approx 4.3$. The average number N of donor electrons interacting with a particular magnetic cation is $(4/3)\pi r_H^3 n_\square$, and the number v of magnetic cations within a donor orbital is $(4/3)\pi r_H^3 x n_O/n$. A somewhat lower value than that given by the hard-sphere approximation is expected in practice, and the threshold will be temperature-dependent[21].

The polaron percolation threshold δ_p and the cation percolation threshold x_p are two landmarks on the magnetic phase diagram (Fig. 3). Provided v is large enough, ferromagnetism occurs when $\delta > \delta_p$ and $x < x_p$. Antiferromagnetism or ferrimagnetism appears beyond x_p where there are continuous paths throughout the crystal joining nearest-neighbour magnetic cations. When $x < x_p$, antiferromagnetic super-exchange cannot create long-range order; at most it will act within small groups of nearest-neighbour cations giving clusters of antiferromagnetically-coupled spins such as ↑↓, ↑↓↑, ……., which reduce the average moment per cation, as seen in Fig. 1.

Table 2 Parameters for some oxides. n_c, cation density; ε, high-frequency dielectric constant; $r_H = \varepsilon(m/m^*)a_0$, hydrogenic radius; v_c, number of cation sites within r_H; δ_p polaron percolation threshold; x_p cation percolation threshold.

Material	Structure	n_c (10^{28} m^{-3})	ε	m^*/m	γ	r_H (nm)	v_c	δ_p (10^{-3})	x_p
ZnO	wurtzite	3.94	4.0	0.28	14	0.76	64	1.5	0.18
TiO_2	anatase	2.93	9.0	1.0	9	0.48	14	5.9	0.25
SnO_2	rutile	2.80	3.9	0.24	16	0.86	75	1.0	0.25

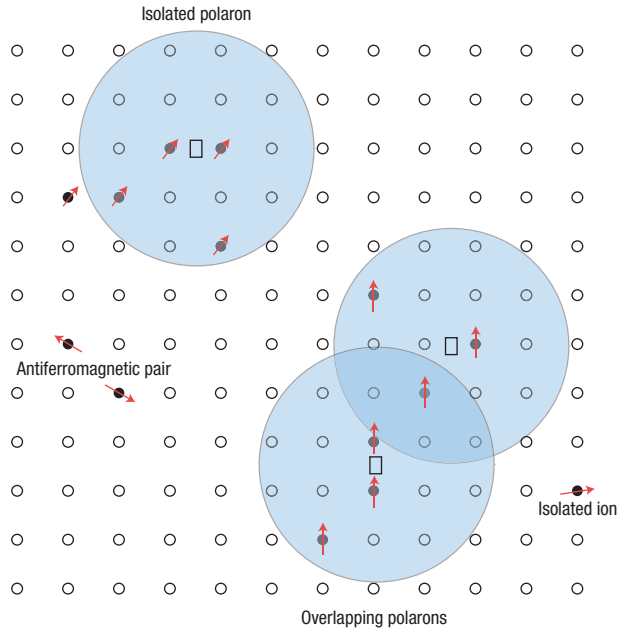

Figure 2 Representation of magnetic polarons. A donor electron in its hydrogenic orbit couples with its spin antiparallel to impurities with a 3*d* shell that is half-full or more than half-full. The figure is drawn for $x = 0.1$, $\gamma = 12$. Cation sites are represented by small circles. Oxygen is not shown; the unoccupied oxygen sites are represented by squares.

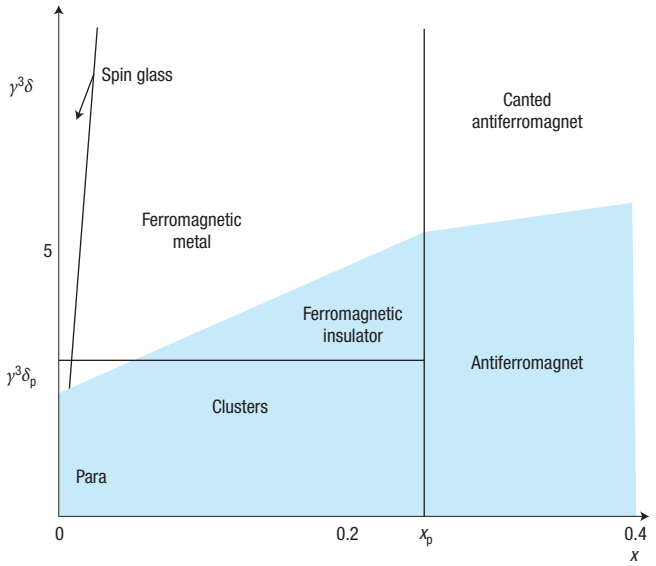

Figure 3 The magnetic phase diagram for dilute ferromagnetic semiconductors. The electrons are localized in the shaded area. x_p and δ_p are the cation and donor polaron percolation thresholds, respectively. γ is the ratio of the radius of the hydrogenic donor orbital to the Bohr radius.

The exchange energy ΔE_{ex} between a localized core spin **S** and a donor electron of spin **s** is given by equation (3) where $\Omega = (4/3)\pi r_c^3$. Here r_c is the cation radius. In the spirit of the hard-sphere approximation, we suppose that $|\psi(r)|^2 = 3/(4\pi r_H^3)$ is a constant when $r < r_H$, and zero otherwise. Hence, $\Delta E_{ex} = -J_{sd}\mathbf{S}.\mathbf{s}/\rho^3$ where $\rho = r_H/r_c$. This interaction can be represented by a molecular field $H_W = J_{sd}\langle \mathbf{S}_z\rangle/2\mu_0\mu_B\rho^3$ acting on the donor electrons, which will be localized provided the impurity band is sufficiently narrow[14]. The electron will be almost completely spin-polarized in the magnetically ordered state if it interacts with many magnetic cations, say $\nu > 10$. The system is analogous to a Néel two-sublattice magnet, where one sublattice is composed of dopant cations, the other of donor electrons. Both are assumed to have a g-factor equal to 2.

The Curie temperature can be estimated in this approximation. The effective field acting on the cation spins **S** is $H_W' = NJ_{sd}\langle \mathbf{s}_z\rangle/2\mu_0\mu_B\rho^3$. Hence

$$\langle \mathbf{S}_z\rangle/\mathbf{S} = B_S(NJ_{sd}\mathbf{S}\langle \mathbf{s}_z\rangle/k_BT\rho^3) \quad (4a)$$

and

$$\langle \mathbf{s}_z\rangle/\mathbf{s} = \tanh(\nu J_{sd}\mathbf{s}\langle \mathbf{S}_z\rangle/k_BT\rho^3). \quad (4b)$$

where $B_S(y)$ is the Brillouin function. Close to T_C, the equations can be linearized using $B_S(y) \approx [(\mathbf{S}+1)/3\mathbf{S}]y$ and $\tanh y \approx y$, yielding

$$T_C = [\mathbf{S}(\mathbf{S}+1)\mathbf{s}^2x\delta n/3]^{1/2}J_{sd}\omega_c/k_B \quad (5)$$

where the cation volume fraction, ω_c (typical value 6%), is the product of cation/anion volume ratio for the oxide and the oxygen packing fraction $f_O \approx 0.74$. Note that T_C is independent of γ. If the donor orbital extends over a sufficient number of cations, there is nothing to be gained by any further increase of the dielectric constant. The electron density $|\psi|^2$ in (3) varies as r_H^{-3} whereas the interaction volume $\nu\Omega$ varies as r_H^3. Exchange coupling with isolated impurities therefore does not alter the size of the hydrogenic orbit, although overlap with antiferromagnetically coupled spins tends to shrink it, and may help localize the states in the impurity band[22].

The Curie temperature can be estimated in a typical case: a monoxide ($n = 1$) with $n_O = 6.10^{28}$ m^{-3}, $x = 0.1$, $\mathbf{S} = 3/2$, $\mathbf{s} = 1/2$, $r_c = 0.06$ nm and $\delta = 0.01$. Derived values are $r_H = 0.8$ nm, $\nu = 13$, $N = 1.3$, and $\rho = 13$, The value of J_{sd} may be inferred for Co in ZnO from the red shift of the band gap with cobalt doping[23] to be 1.5 eV. The Curie temperature given by equation (5) is then $T_C = 18$ K. Positional disorder of the impurities may enhance T_C somewhat [24], but the estimate is too low by one or two orders of magnitude.

Delocalizing the donor electrons reduces T_C. Equation (4b) is then replaced by $\langle \mathbf{s}_z\rangle/\mathbf{s} = \nu J_{sd}\mathbf{s}\langle \mathbf{S}_z\rangle/\varepsilon_F\rho^3$ where ε_F is the Fermi energy in the impurity band, and the expression for T_C becomes

$$T_C = \mathbf{S}(\mathbf{S}+1)\mathbf{s}^2nx\delta J_{sd}^2\omega_c^{2/3}/k_B\varepsilon_F \quad (6)$$

The value of T_C in the example is then <1 K, if $\varepsilon_F = 0.1$ eV. Expressions similar to equations (5) and (6) have been given in a discussion[25] of the magnetization of dilute magnetic semiconductors such as $(Ga_{1-x}Mn_x)As$. Magnetic polarons in that system are thought to form around some Mn sites. They are coupled to surrounding Mn ions by an exponentially decaying exchange interaction, and the Curie temperature is the point where the extended clusters percolate[21]. We simplify the problem by considering the magnetic polarons around the donor electrons in the impurity band as uniformly magnetized spheres, calculating their magnetization from equation (4b), which is justified when most states in the impurity band are localized.

The only option for boosting T_C significantly is somehow to increase the donor electron density $|\psi|^2$ in the vicinity of the magnetic impurities. An upper limit, $\nu\Omega|\psi|^2 < 1$, is obtained by distributing the donor electrons entirely around the impurities. In the example, this gives $T_C < 3{,}600$ K. The observed values of T_C

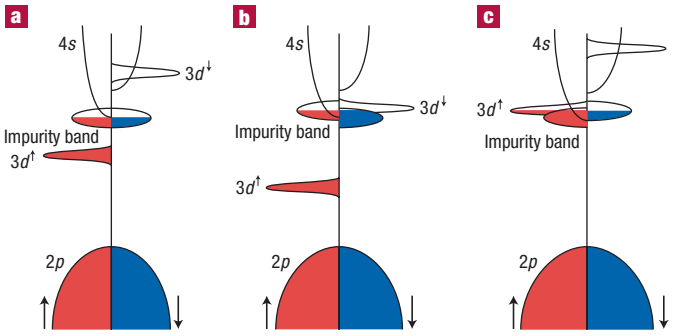

Figure 4 Schematic band structure of an oxide with 3*d* impurities and a spin-split donor impurity band. **a**, The position of the 3*d* level for low Curie temperature T_C, when the splitting of the impurity band is small. **b**, and **c**, show positions of the minority (**b**) or majority-spin (**c**) 3*d* bands, respectively, which lead to high T_C.

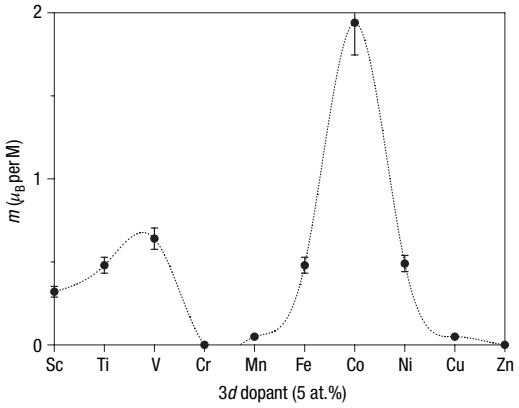

Figure 5 The magnetic moment of thin films produced from $(Zn_{0.95}M_{0.05})O$ targets by pulsed-laser deposition, for M = Sc – Cu, measured at room-temperature. The moment is expressed in Bohr magnetons per M ion. Maxima occur when there is a large density of $d^{\uparrow}$ or $d^{\downarrow}$ states at the Fermi level, which is pinned in the donor impurity band. Relative errors shown are based on the uncertainties in film thickness and composition.

require about 15% of the donor charge density to be redistributed over the impurity sites.

In order to transfer the necessary ~1–2% of an electron from the donor states to each magnetic cation, instead of just $\rho^{-3} = (r_c/r_H)^3 \approx 0.04\%$ in the uniform case, empty 3*d* states ($3d^{\downarrow}$ in the example of a $3d^7$ impurity; $\mathbf{S} = 3/2$) have to hybridize with the donor states at the Fermi level. The exchange splitting of the impurity band $2\mu_B\mu_0 H_w$ is then $J_{sd}\langle \mathbf{S}_z\rangle/\rho^3$.The electron transfer effect may be represented by introducing a factor $(r_c^{eff}/r_c)^3$ in equation (5), which becomes

$$T_C = [(\mathbf{S}+1)\mathbf{s}^2 x\delta/3n]^{1/2} J_{sd} f_O (r_c^{eff}/r_O)^3/k_B \qquad (7)$$

With $r_O = 0.14$ nm, if $T_C \sim 500$ K in the example, the effective cation radius is $r_c^{eff} = 0.20$ nm. In other words, J_{sd} is rescaled by a factor $(r_c^{eff}/r_O)^3$. The electronic structure necessary for a high Curie temperature is contrasted with that for a low Curie temperature in Fig. 4. On passing along the 3*d* series from Ti to Cu, the spin-split *d*-levels move down in energy towards the top of the oxygen 2*p*-band[26]. Hence there are two regions where a high T_C is expected: one near the beginning of the series where the $3d^{\uparrow}$ states cross the Fermi level in the impurity band, and one towards the end where the $3d^{\downarrow}$ states cross the Fermi level. There is evidence of the former in reports of high T_C for V in ZnO (ref. 27) and TiO_2 (ref. 28). We have examined thin films of ZnO doped with every element in the 3*d* series from Sc to Cu. Films were deposited from targets of $(Zn_{0.95}M_{0.05})O$ by pulsed-laser deposition. The room-temperature moment in μ_B per dopant cation is plotted in Fig. 5, where the two distinct peaks appear, one at Ti and V, the other at Co. Moments are near zero for Cr, Mn and Cu. It is remarkable that ferromagnetism is observed for Sc in ZnO, a d^0 system. We have observed d^0 ferromagnetism in other materials, including undoped films of HfO_2 (ref. 29).

RKKY EXCHANGE

As δ increases, there comes a point where the impurity-band model breaks down, and the donor states merge with the bottom of the conduction band. It is then appropriate to think of RKKY (Ruderman–Kittel–Kasuya–Yosida) exchange. This interaction is operative even when the Fermi level lies below the mobility edge, provided the separation of magnetic cation neighbours is less than the localization length. The Fermi wavevector k_F is small at the bottom of the band, and the RKKY interaction is always ferromagnetic at low electron densities. At higher densities, the interaction will provide as many negative as positive exchange bonds, and the system becomes a spin glass. The first change of sign of the RKKY function $F(\xi) = -[(\xi\cos(-\sin\xi)/\xi^4]$ is at $\xi = 2k_F r = 2.87$, where k_F is the Fermi wavevector $(3\pi^2 n_{\square})^{1/3}$. In a free-electron band the corresponding condition for ferromagnetism $x > 2.6n\delta$, is easily satisfied. The Curie temperature in the molecular field approximation considering only *z* nearest-neighbour sites is $T_C = 2zJ_{RKKY}\mathbf{S}(\mathbf{S}+1)/3k_B$ where J_{RKKY} is given by the expression[30] $[(J_{sd}^2 m^* k_F^4 n^2)/(32\pi^3\hbar^2 n_O^2)]F(\xi)$. In the small-$\xi$ limit, $F(\xi) \approx 1/3\xi$, hence

$$T_C \approx zJ_{sd}^2\mathbf{S}(\mathbf{S}+1)m^*\delta(n^5 x/n_O^2)^{1/3}/(48\pi\hbar^2 k_B) \qquad (8)$$

Taking $z = 12$, $m^*/m = 1$, and the same values for J_{sd}, **S**, *n*, *x* and δ as before, we find $F(\xi) = 0.116$, $J_{RKKY} = 0.52$ K and $T_C = 16$ K. In order to enhance the interaction, it would again be necessary to transfer conduction-band electrons to the 3*d* impurities, but this is precluded for the second half of the 3*d* series if the spin polarization of the conduction band is positive. The RKKY model is readily distinguished from the magnetic polaron impurity-band model by the sign of the splitting of the conduction-band edge for magnetic impurities with a 3*d* shell that is half full or more (Fig. 4).

ORIGIN OF THE MOMENTS

The nature of the defects responsible for the shallow donors has been unspecified so far. Their job is to provide *n*-type conduction. Oxygen vacancies at the percent level are documented for the higher oxides SnO_2 and TiO_2 (ref. 31), and also for ZnO (ref. 32), where Zn interstitials are also found. In nitrides, extended defects may play the role of donors in establishing a spin-polarized impurity band. Doubly occupied vacancies (F^0 centres) are shallow donors, but they form a $1s^2$ singlet state which only mediates weak antiferromagnetic exchange. Overlap with the 4*s* band, or partial compensation would remove some electrons from the impurity band, and favour ferromagnetism. Singly occupied vacancies (F^+ centres) lie deep in the gap.

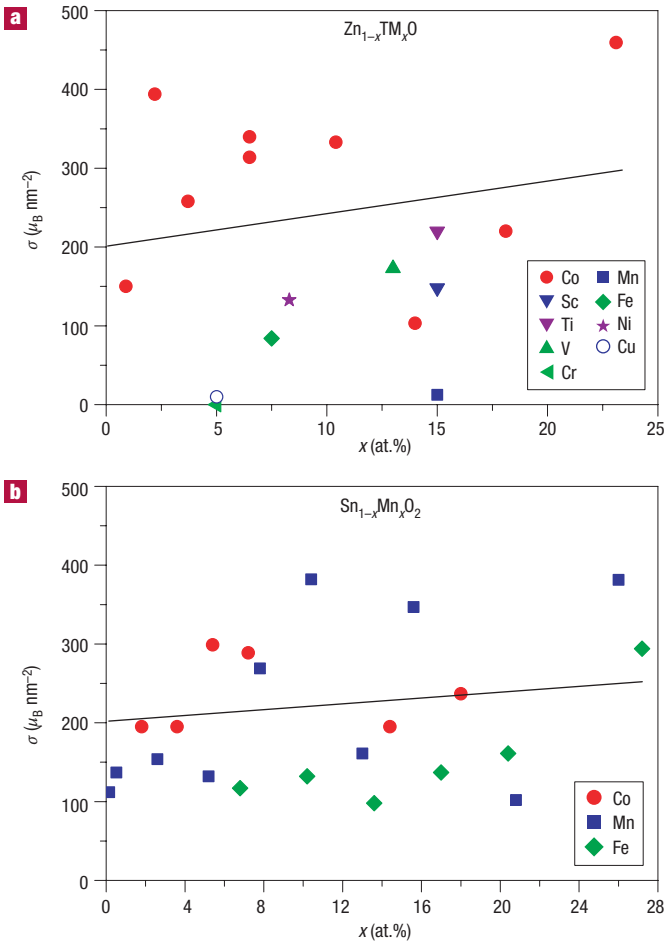

Figure 6 Magnetic moments measured on thin films of doped ZnO or SnO_2 expressed in Bohr magnetons per unit substrate area. The data extrapolate to a non-zero value of approximately 200 μ_B nm^{-2}. It seems that there is a moment associated with defects in these films, which is 'activated' by the magnetic dopants.

Finally, we return to the issue of d^0 ferromagnetism. In terms of the model, it might arise when the impurity band overlaps an empty $d^{\uparrow}$ band, leading to some charge transfer as indicated in Fig. 4c. However, there is growing evidence of another source of magnetism in dilute magnetic oxide films, besides the cations with *d*-electron character. The tell-tale symptom is that the moment per cation can exceed the spin-only value in the dilute limit. Examples are shown in Fig. 1. Extrapolating the moment versus cation concentration or film thickness gives ~200 μ_B per square nanometre for a thin, undoped film (Fig. 6). This suggests that defects introduced at film/substrate interface are always involved. Two-electron defects that have a triplet ground state or low-lying triplet excited state are the V^0 centre (a cation vacancy) and the F_t centre (adjacent F^+ centres)[33]. The average defect separation in a 10-nm film or defective interface layer is about 0.5 nm, so the triplet molecular orbitals may themselves form an impurity band, taking the place of the magnetic polarons discussed previously. The impurity band could split spontaneously if narrow enough, or be polarized by exchange with 3*d* cations when these are present. Such a model is needed at low dopant concentrations, $x \leq 1\%$.

In conclusion, the syndrome associated with high-temperature ferromagnetism in dilute magnetic oxides has been analysed in terms of a model of indirect exchange via shallow donors, treated in a two-sublattice mean-field approximation. High Curie temperatures require hybridization and charge transfer from a donor-derived impurity band to unoccupied 3*d* states at the Fermi level. Predictions regarding the sign and magnitude of the spin splitting of the conduction band (red shift of the bandgap) below T_C, the variation of T_C with donor concentration δ and magnetic impurity concentration *x*, as well as the position of the impurity in the 3*d* series and the possibility of ferromagnetism in d^0 oxides can all be tested experimentally, and the results used to refine the model. The model also suggests how interactions may be tuned by compensation. It should help advance the arrival of the first ferromagnetic semiconductors with useful room-temperature functionality.

Received 11 May 2004; accepted 29 November 2004; published 16 January 2005.

References

1. Prellier, W., Fouchet, A. & Mercey, B. Oxide-diluted magnetic semiconductors: a review of the experimental status. *J. Phys. Condens. Matter* **15,** R1583–R1601 (2003).
2. Pearton, S. J. *et al.* Wide band gap ferromagnetic semiconductors and oxides *J. Appl. Phys.* **93,** 1–13 (2003).
3. Dietl, T. *et al.* Zener model description of ferromagnetism in zinc-blende magnetic semiconductors. *Science* **287,** 1019–1022 (2000).
4. Matsumoto, Y. *et al.* Room-temperature ferromagnetism in transparent transition metal-doped titanium dioxide *Science* **291,** 854–856 (2001).
5. Ueda, K., Tabata, H. & Kawai, T. Magnetic and electric properties of transition-metal-doped ZnO films. *Appl. Phys. Lett.* **79,** 988–990 (2001).
6. Ogale, S. B. *et al.* High temperature ferromagnetism with a giant magnetic moment in transparent Co-doped $SnO_{2-\delta}$. *Phys. Rev. Lett.* **91,** 077205 (2003).
7. Kim, J. Y. *et al.* Ferromagnetism induced by clustered Co in Co-doped anatase TiO_2 thin films *Phys. Rev. Lett.* **90,** 017401 (2003).
8. Punnoose, A., Seehra, M. S., Park, W. K. & Moodera, J. S. On the room temperature ferromagnetism in Co-doped TiO_2 films. *J. Appl. Phys.* **93,** 7867–7869 (2003).
9. Rode, K. *et al.* Magnetic semiconductors based on cobalt substituted ZnO. *J. Appl. Phys.* **93,** 7676–7678 (2003).
10. Ramachandran, S., Tiwari, A. & Narayan, J. $Zn_{0.9}Co_{0.1}O$-based diluted magnetic semiconducting thin films. *Appl. Phys. Lett.* **84,** 5255–5257 (2004).
11. Goodenough, J. B. *Magnetism and the Chemical Bond* (Interscience, New York, 1963).
12. Holtzberg, F., von Molnar, S. & Coey, J. M. D. *Handbook on Semiconductors* Vol. 3 (ed. Keller, S.) 850 (North Holland, Amsterdam, 1980).
13. Dietl, T. Ferromagnetic semiconductors. *Semicond. Sci. Technol.* **17,** 377–392 (2002).
14. Mott, N. F. *Conduction in Noncrystalline Materials* (Oxford Univ. Press, Oxford, 1987).
15. von Molnar, S. & Kasuya, T. in *Proceedings of 10th International Conference on Physics of Semiconductors* (eds Keller, S. P., Hensel, J. C. & Stern, F.) 233 (U.S.A.E.C. Division of Technical Information, Springfield, Vancouver, 1970).
16. Dietl, T. & Spalek, J. J. Effect of thermodynamic fluctuations of magnetization on the bound magnetic polaron in dilute magnetic semiconductors. *Phys. Rev. B* **28,** 1548–1563 (1983).
17. Wolff, P. A. *Semiconductors and Semimetals* Vol. 25 (eds Furdyna, J. R. & Kossut, J.) (Academic, San Diego 1988).
18. Angelescu, D. E. & Bhatt, R. N. Effective interaction Hamiltonian of polaron pairs in diluted magnetic semiconductors. *Phys. Rev. B* **65,** 075211 (2002).
19. Durst, A. C., Bhatt, R. N. & Wolff, P. A. Bound magnetic polaron interactions in insulating doped diluted magnetic semiconductors. *Phys. Rev. B* **65,** 235205 (2002).
20. Zallen, R. M. *Physics of Amorphous Solids* (Wiley, New York, 1983).
21. Kaminski, A. & Das Sarma, S. Polaron percolation in diluted magnetic semiconductors. *Phys. Rev. Lett.* **88,** 247202 (2002).
22. Kasuya, T. Mobility of antiferromagnetic large polaron. *Solid State Commun.* **8,** 1635 (1970).
23. Kim, K. J. & Park, Y. R. Spectroscopic ellipsometry study of optical transitions in $Zn_{1-x}Co_xO$ alloys. *Appl. Phys. Lett.* **81,** 1420–1422 (2002).
24. Berciu, M. & Bhatt, R. N. Effects of disorder on ferromagnetism in diluted magnetic semiconductors. *Phys. Rev. Lett.* **87,** 107203 (2001).
25. Das Sarma, S., Hwang, E. W. & Kaminski, A. Temperature-dependent magnetization in diluted magnetic semiconductors. *Phys. Rev. B* **67,** 155201 (2003).
26. Wilson, J. A. Systematics of breakdown of Mott insulation in binary transition-metal compounds. *Adv. Phys.* **21,** 143 (1972).
27. Saeki, H., Tabata, H. & Kawai, T. Magnetic and electric properties of vanadium doped ZnO films. *Solid State Commun.* **120,** 439–443 (2001).
28. Hong, N.Y H., Sakai, J. & Hassini, A. Ferromagnetism at room temperature with a large magnetic moment in anatase V- doped TiO_2 thin films. *Appl. Phys. Lett.* **84,** 2602–2604 (2004).
29. Venkatesan, M., Fitzgerald, C. B. & Coey, J. M. D. Unexpected magnetism in a dielectric oxide. *Nature* **430,** 630–630 (2004).
30. Mattis, D. C. *Theory of Magnetism* Vol. 1 (Springer, Berlin, 1981).
31. Yahia, J. Dependence of electrical conductivity and thermoelectric power of pure and aluminium-doped rutile on equilibrium oxygen pressure and temperature. *Phys. Rev.* **130,** 1711–1719 (1963).
32. Kohan, A. F., Ceder, G., Morgan, D. & Van de Walle, C. G. First-principles study of native point defects in ZnO. *Phys. Rev. B* **61,** 15019–15027 (2000).
33. Stoneham, A. M. *Theory of Defects in Solids* Ch. 16 (Clarendon, Oxford 1975).
34. Sonoda, S., Shimizu, S., Sasaki, T., Yamamoto, Y. & Hori, H. Moleclar beam epitaxy of wurtzite (Ga,Mn)N films on sapphire (0001) showing the ferromagnetic behaviour at room temperature. *J. Cryst. Growth* **237,** 1358–1362 (2002).

35. Hashimoto, M., Zhou, Y. K., Kanamura, M. & Asahi, H. High-temperature (>400K) ferromagnetism in III-V based diluted magnetic semiconductor GaCrN grown by ECR molecular-beam epitaxy. *Solid State Commun.* **122,** 37–39 (2002).
36. Wu, S. Y. *et al.* Synthesis, Characterization and modeling of high-quality ferromagnetic Cr-doped AlN thin films. *Appl. Phys. Lett.* **82,** 3047–3049 (2003).
37. Shinde, S. R. *et al.* Ferromagnetism in laser-deposited anatase $Ti_{1-x}Co_xO_{2-\delta}$ films. *Phys. Rev B* **67,** 115211 (2003).
38. Wang, Z. J., Tang, J. K., Tung, L. D., Zhou, W. L. & Spinu, L. Ferromagnetism and transport properties of Fe-doped reduced-rutile $TiO_{2-\delta}$ films. *J. Appl. Phys.* **93,** 7870–7872 (2003).
39. Coey, J. M. D., Douvalis, A. P., Fitzgerald, C. B. & Venkatesan, M. Ferromagnetism in Fe-doped SnO_2 films. *Appl. Phys. Lett.* **84,** 1332–1334 (2004).
40. Sharma, P. *et al.* Ferromagnetism above room temperature in bulk and transparent thin films of Mn-doped ZnO. *Nature Mater.* **2,** 673–677 (2003).
41. Han, S. J. *et al.* Magnetism in Mn-doped ZnO bulk samples prepared by solid-state reaction. *Appl. Phys. Lett.* **83,** 920–922 (2003).
42. Radovanovic, P. V. & Gamelin, D. R. High-temperature ferromagnetism in Ni^{2+}-doped ZnO aggregates prepared from colloidal diluted magnetic semiconductor quantum dots. *Phys. Rev. Lett.* **91,** 157202 (2003).
43. Kale, S. N. *et al.* Magnetism in cobalt-doped Cu2O thin films without and without Al, V and Zn codopants. *Appl. Phys. Lett.* **83,** 2100–2102 (2003).
44. Philip, J., Theodoropolou, N., Berera, G., Moodera, J. S. & Satpati, B. High-temperature ferromagnetism in manganese-doped indium-tin oxide films. *Appl. Phys. Lett.* **85,** 777–779 (2004).

Acknowledgements

This work was supported by Science Foundation Ireland as part of the CINSE project. The authors are grateful to James Lunney, Sebastiaan van Dijken, Stefano Sanvito and Plamen Stamenov for their helpful comments.
Correspondence and requests for materials should be addressed to J.M.D.C.

Competing financial interests

The authors declare that they have no competing financial interests.